THE JOURNAL OF PHYSICAL CHEMISTRY B

Article

pubs.acs.org/JPCB

Understanding the Interaction of Block Copolymers with DMPC Lipid Bilayer Using Coarse-Grained Molecular Dynamics Simulations

Samira Hezaveh,[†] Susruta Samanta,[†] Antonio De Nicola,[‡,§] Giuseppe Milano,*[,‡,§] and Danilo Roccatano*[,†]

[†]Jacobs University Bremen, Campus Ring 1, D-28759 Bremen, Germany

[‡]Dipartimento di Chimica e Biologia and NANOMATES, Research Centre for NANOMAterials and nanoTEchnology at Università di Salerno, I-84084 via Ponte don Melillo Fisciano (SA), Italy

[§]IMAST Scarl-Technological District in Polymer and Composite Engineering, P. le Fermi 1, 80055 Portici (NA), Italy

Supporting Information

ABSTRACT: In this paper, we present a computational model of the adsorption and percolation mechanism of poloxamers (poly(ethylene oxide) (PEO) and poly(propylene oxide) (PPO) triblock copolymers) across a 1,2-dimyristoyl-*sn*-glycero-3-phosphocholine (DMPC) lipid bilayer. A coarse-grained model was used to cope with the long time scale of the percolation process. The simulations have provided details of the interaction mechanism of Pluronics with lipid bilayer. In particular, the results have shown that polymer chains containing a PPO block with a length comparable to the DMPC bilayer thickness, such as P85, tends to percolate across the lipid bilayer. On the contrary, Pluronics with a shorter PPO chain, such as L64 and F38, insert partially into the membrane with the PPO block part while the PEO blocks remain in water on one side of the lipid bilayer. The percolation of the polymers into the lipid tail groups reduces the membrane thickness and increases the area per lipid. These effects are more evident for P85 than L64 or F38. Our findings are qualitatively in good agreement with published small-angle X-ray scattering experiments that have evidenced a thinning effect of Pluronics on the lipid bilayer as well as the role of the length of the PPO block on the permeation process of the polymer through the lipid bilayer. Our theoretical results complement the experimental data with a detailed structural and dynamic model of poloxamers at the interface and inside the lipid bilayer.

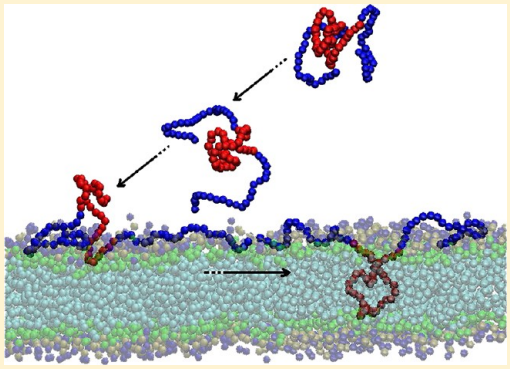

INTRODUCTION

Poloxamers (also known as their trademark name, Pluronics) are amphiphilic linear ABA-type triblock copolymers with the B block composed of hydrophobic poly(propylene oxide) (PPO) and the two A blocks of hydrophilic poly(ethylene oxide) (PEO) homopolymers. They have broad range of biomedical applications.[1−8] They are used, for example, as drug delivery systems,[9−11] in gene and cancer therapies.[12,13] These broad ranges of applications are result of their peculiar properties in solutions and at biological interfaces. In particular, by changing the length of the polymer blocks, their solubility and other solution thermodynamic properties can be customized for specific applications.[14]

For drug delivery, hydrophobic drugs are embedded in block copolymer micelles to prevent their rapid turnover by increasing their biocompatibility and solubility. The drug release at cellular level involves molecular interaction mechanisms of the polymers with the membranes. The dynamics at atomic level of these processes is so far not easily accessible to experimental measurements and therefore many questions are still undisclosed on the molecular details of the interaction mechanisms.

Many experimental studies have been focused on the percolation capability of these polymers into lipid mono- and bilayer systems.[15−22] From these studies, it is clear that the interaction of polymers with lipid layers is strongly influenced by the hydrophilic−lipophilic balance (HLB) caused by PEO/PPO block length ratio.[23] For instance, Pluronics with low HLB ratio (i.e., very large PPO block compared to the PEO blocks) can assist the permeation of small molecules through lipid bilayers,[2] show ionophoric activity,[24] act as chemo-sensitizing agents in cancer treatments,[25] and in some cases, they can even enter the cell.[23] On the other hand, Pluronics with large HLB ratio (i.e., large PEO blocks), being too hydrophilic, are unable to bind strongly across cell membranes and their interaction is limited to the coating of the cellular membrane surfaces.[23] Simple model membrane systems, such as lipid Langmuir monolayers, liposomes, giant unilamellar vesicles, and planar bilayers, have been investigated using different variety of techniques such as X-ray and neutron scattering methods[26,27] calorimetric measurements,[19,28,29] fluorescence microscopy,[19,30,31] and other microscopy techniques.[6] These studies have evidenced that the nature of the interaction mainly

Received: July 3, 2012
Revised: November 2, 2012
Published: November 8, 2012

dx.doi.org/10.1021/jp306565e | *J. Phys. Chem. B* 2012, 116, 14333−14345

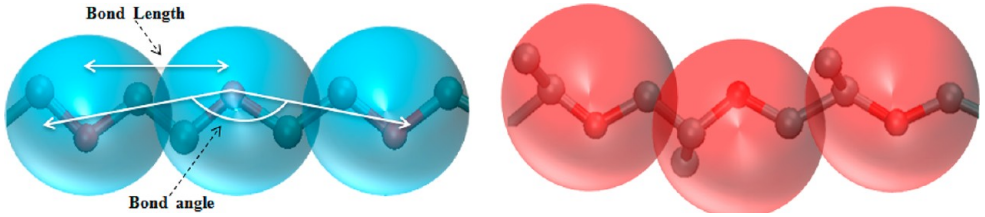

Figure 1. PEO (left) and PPO (right) mapping scheme from atomistic to CG MARTINI model.

Table 1. CG Force Field Parameters for Bonded and Nonbonded Interactions Used in This Work to Model PEO and PPO Polymers

PEO Bonded Parameters			
bond		angle	
b (nm)	K (kJ mol^{-1}nm^{-2})	θ (deg)	K (kJ mol^{-1})
0.28	8000	155	40
PEO Nonbonded Parameters			
	σ (nm)	ε (kJ mol^{-1})	
PEO-PEO	0.48	3.5	
PEO-W	0.47	4.5	
PPO Bonded Parameters			
bond		angle	
b (nm)	K (kJ mol^{-1}nm^{-2})	θ (deg)	K (kJ mol^{-1})
0.28	5000	140	40
PPO Nonbonded Parameters			
	σ (nm)	ε (kJ mol^{-1})	
PPO-PPO	0.50	2.6	
PPO-W	0.47	3.5	
Other Nonbonded Parameters			
	σ (nm)	ε (kJ mol^{-1})	
PEO-PPO	0.47	2.9	
W−W	0.47	5.0	

depends on the length of PPO block compared to the bilayer thickness. In fact, the PPO block has a stronger affinity to the hydrophobic tails of the lipid bilayer than the PEO blocks that prefer to stay outside in contact with the hydrophilic head groups.[9,32,33] Therefore, Pluronics with PPO block lengths less than the thickness of the bilayer insert partially into the hydrophobic region of membrane while those with PPO lengths comparable with the hydrophobic thickness of bilayer can completely span across the membrane with their PEO blocks flanking in water in the opposite sides of the bilayer.[9] Unfortunately, these pieces of experimental evidence do not provide the details of dynamics and molecular mechanism of these processes.[34] These information can be easily obtained with molecular modeling, in particular with molecular dynamics (MD) simulations. So far, several computational studies have been conducted on Pluronics at different levels of scale.[35−40] However, to the best of our knowledge, none of these theoretical studies have addressed the interaction mechanism of Pluronics with DMPC lipid bilayers. This lack of detailed atomistic model of this process gave us the motivation for the study reported in this paper. We have used MD simulations at the coarse-grained (CG) level of scale to study the interaction of Pluronic chains of different PEO and PPO block lengths with a DMPC lipid bilayer. The use of CG MD simulations was necessary to cope with the time scale of spontaneous diffusion of the polymers in the lipid bilayer that it goes beyond the capability of ordinary full atomistic simulations.

Table 2. Description of the Pluronics Block Lengths Used in This Study

	no. PEO blocks	no. PPO blocks
P85	26	40
L64	13	30
F38	43	15

Table 3. Summarized Information of the Systems Simulated for Single Chain of Pluronics in Random Mixture and on the Top of Bilayer Surface

	ternary mixture			bilayer		
single chain	box size (nm)	waters	lipids	box size (nm)	waters	lipids
P85	8.5	5540	300	10	7400	300
L64	8.5	5540	300	10	7400	300
F38	8.5	5540	300			

Table 4. Summarized Information of the Systems Simulated for Multichains of Pluronics in Random Mixture and on the Top of Bilayer Surface

	ternary mixture			bilayer		
polymer	box size (nm)	water	lipids	box size (nm)	water	lipids
P85	9.5	6400	310	10	7379	287
L64	9.5	6400	310	10	7379	287

Table 5. Radius of Gyration Values for Pluronics in Water at 293 K

	R_g (nm)		
	L64	P85	F38
Pluronic	1.68 ± 0.08	2.19 ± 0.20	3.25 ± 0.22
PPO	1.03 ± 0.10	1.15 ± 0.31	0.82 ± 0.01

The MARTINI CG model was adopted for this study to provide insights on the mechanism of this process. The results of the study have been compared with the experimental SAXS data from Firestone et al.[9,33] The authors of these experimental papers proposed different interaction models by comparing the periodicity of the diffraction peaks from a DMPC−water−Pluronics mixture with the one from the pure DMPC−water system. The results of our simulations resulted in good agreement with these experimental data.

The paper is organized as follows: the details of the force field parametrization for the CG model of the Pluronics are reported in the Supporting Information. The force field parameters for the Pluronics were validated by calculating the radii of gyration (R_g) for PEO and PPO chains of different lengths in water and comparing them with those from experimental measurements[41] and atomistic models.[42] The Results and Discussion section is organized in two parts. In the first part, the results of the Pluronics L64, P85, and F38 simulations in water are reported. In the second

dx.doi.org/10.1021/jp306565e | J. Phys. Chem. B 2012, 116, 14333−14345

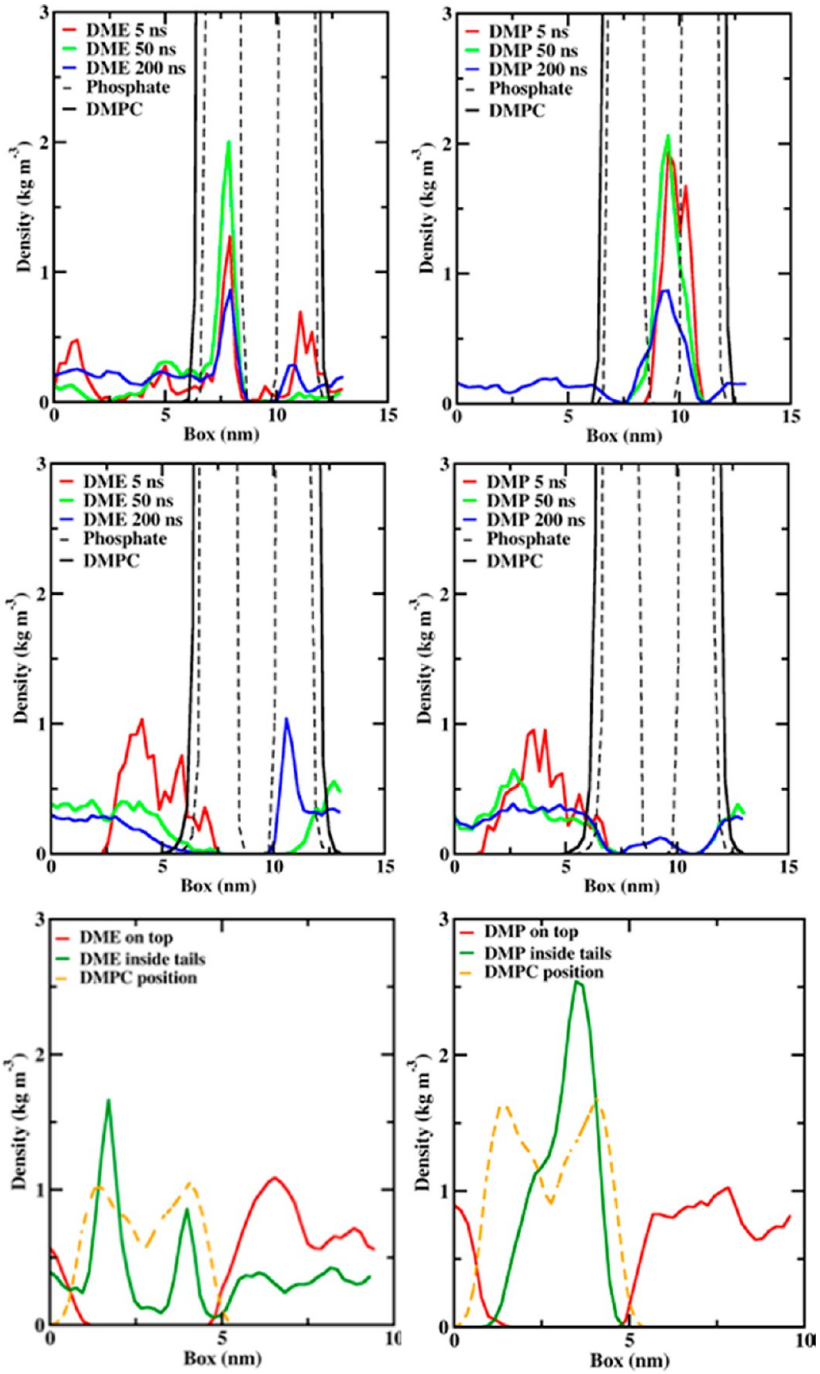

Figure 2. Density profiles for single DME (first column) and DMP (second column). The profiles for DME/DMP in the lipid tails region (top row) and those for the same molecules on top of DMPC bilayer (middle row) at 310 K are shown. The results for atomistic simulations[50] are reported in the last row for comparison.

part, simulations of three different Pluronics with the DMPC lipid bilayer are presented. These simulations have been performed for Pluronics−DMPC−water ternary mixtures and for Pluronics in water at the interface of preformed DMPC lipid bilayer. Finally, in the Conclusions section, the main results of this study are summarized.

METHODS

Force-Field Parametrization. The CG models used for MD simulations of polymers and lipids are based on the MARTINI force field.[43,44] The model parameters for the polymers were optimized based on an atomistic model of the same polymers recently proposed by our group.[42,45] The mapping scheme of the CG bead is the same as those adopted by similar CG model of PEO proposed by other groups.[36,37] Each bead of the CG model for PEO and PPO includes three (C−O−C) and four ($C(CH_3)$−O−C) heavy atoms, respectively. Oxygen atoms were considered the center of each bead for both polymers. From the atomistic simulations, the bond length and bond angle distributions were calculated considering the distance between oxygen atoms of two consecutive monomers and the angle formed by the two adjacent distance vectors as shown in Figure 1. Detailed information on CG force field parametrization and

dx.doi.org/10.1021/jp306565e | J. Phys. Chem. B 2012, 116, 14333−14345

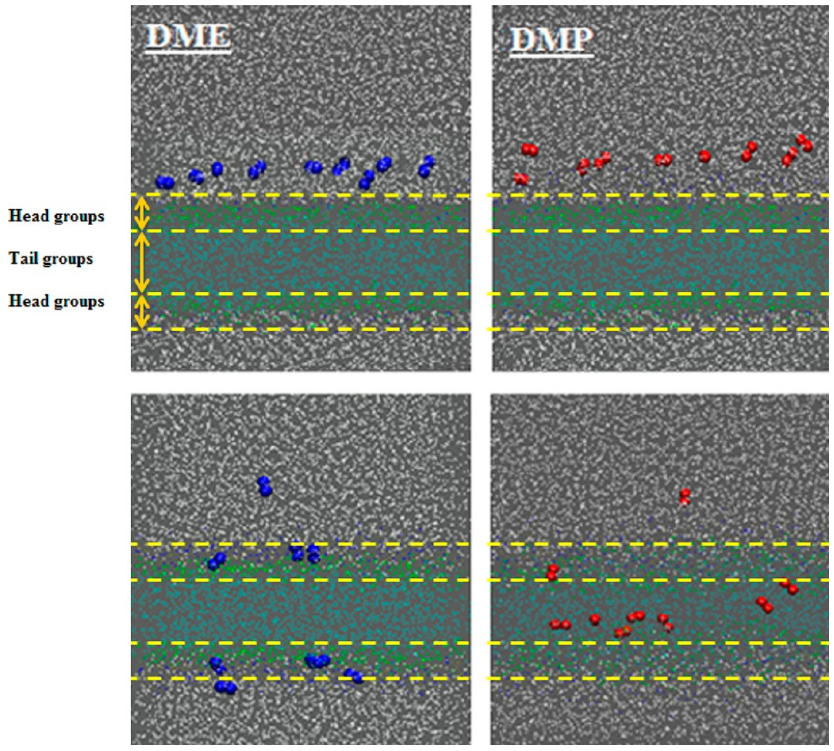

Figure 3. Snapshots of simulations of nine DME/DMP on top of DMPC bilayer at 0 ns (top row) and 400 ns (bottom row). White points are water molecules. The bilayer tail- and head-group regions are within the range indicated with arrows. DMEs/DMPs are shown in blue and red, respectively.

validation are available in the Supporting Information and the final optimized parameters are reported in Table 1.

As for the models proposed by Lee et al. (for PEO)[36] and Hatakeyama and Faller (for PEO and PPO),[39] we have also used the constant bead mass of 72 amu for efficiency reasons.[39,43] Therefore, our model does not properly scale mass-dependent properties because the real masses of PEO and PPO monomers are 44 and 58 amu, respectively. For these properties, only qualitative comparisons can be made with experimental data.

A comparison between nonbonded Lennard-Jones (LJ) parameters obtained by us and those reported by Lee et al.[36] for PEO shows slight differences. But there are noticeable differences in the reference geometric parameters for bonds and bond angles and also absence of proper dihedrals in our model. The variations are probably due to the different reference atomistic models used for the parametrization. Concerning the PPO CG model, Hatakamaya and Faller[39] have proposed a MARTINI based model for study of Pluronics. However, they did not follow the mapping procedure from atomistic to CG model and bonded and nonbonded parameters of our PPO model are completely different from their values. So far and to the best of our knowledge, other models of the PPO based on MARTINI force field have not been reported in the literature.

Simulation Setup. All MD simulations were performed using GROMACS (version 4.0.7) software package.[46] A cutoff of 12 Å was applied for LJ and Coloumbic interactions. The LJ potential was smoothly shifted to zero between 0.9 and 1.2 nm, and the Coulomb potential was smoothly shifted to zero between 0.0 and 1.2 nm. The temperature and pressure were maintained to the reference values (for the pressure, P_0 = 1 bar) using the Berendsen thermostat and barostat[47] with coupling time constant of τ_T = 0.3 ps for temperature and τ_p = 3.0 ps for the pressure. A time step of 30 fs was used. All errors on the calculated properties have been evaluated using the block averaging method.[48]

Simulation of Pluronics. Pluronics L64, P85, and F38 were chosen for the simulations (see Table 2 for details). Each polymer was simulated at 293 K for ∼900 ns in a simulation box of ∼9 nm/side containing ∼7600 water molecules. The radius of gyration of P85 was compared with the experimental value measured at the same temperature.[49]

Simulation of 1,2-Dimethoxyethane (DME) and 1,2-Dimethoxypropane (DMP) with DMPC Lipid Bilayer. Simulations of single DME/DMP inside the tail groups and on top of lipid bilayer were performed at 310 K for 200 ns in a box of 10 nm/side containing ∼7400 water molecules. Another set of simulation was performed for nine molecules of each oligomer on top of the lipid bilayer for 400 ns at 310 K in a box of the same size. The bilayer used for both setups consisted of 300 phospholipid molecules.

Simulations of Pluronics with DMPC Bilayer. Two sets of simulations have been performed at 310 K. In the first set, the random conformation of one polymer chain was solvated in a mixture of DMPC lipid/water; in the second set, the Pluronic chains were positioned on the water phase on the top of an equilibrated DMPC lipid bilayer. The details for two sets of simulations are as follows:

(a) *Single Chain.* One chain of each Pluronic L64, P85, and F38 was positioned in the simulation box and then the DMPC lipid chains were randomly positioned in the box while the remaining volume was filled with water molecules. In the second set, L64 and P85 Pluronic chains were positioned at a distance of 1−2 nm on the top of an equilibrated DMPC lipid bilayer in water (see Table 3 for details).

(b) *Multiple Chains.* Five chains of Pluronic L64 and P85 were positioned randomly in simulation boxes and then DMPC lipids were randomly positioned. For the Pluronics at DMPC interface,

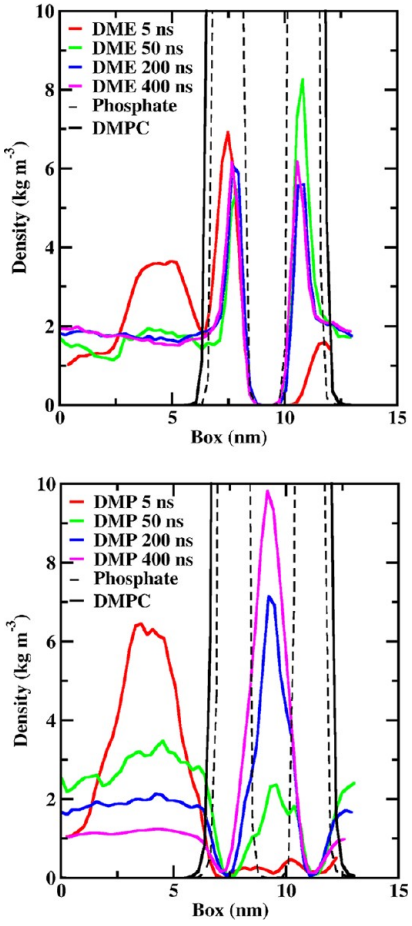

Figure 4. Density profiles for nine DME/DMP molecules on the top of DMPC bilayer at 310 K.

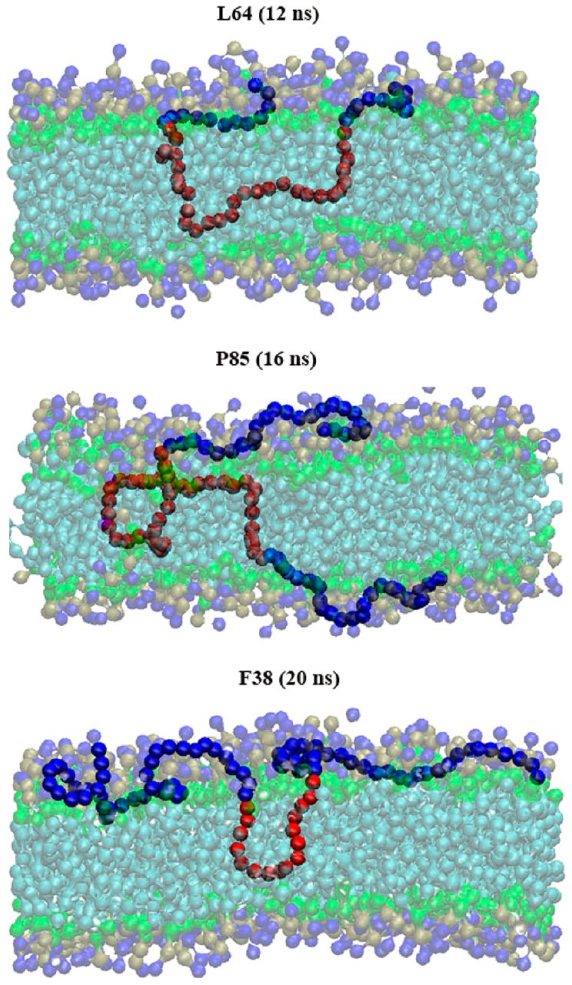

Figure 5. Interactions of Pluronics (different PPO block lengths) with DMPC bilayer at 310 K. The snapshots were taken right after bilayer formation. Numbers in parentheses show the time needed for the bilayer formation. For clarity, water molecules are not shown.

the setup was repeated in the same way as for the single-chain simulation with five chains on top of the lipid bilayer (see Table 4 for details).

RESULTS AND DISCUSSION

Pluronics in Water. Simulations were performed for three Pluronics, L64, P85, and F38, at 293 K. The R_g of the polymers are reported in Table 5. R_g of P85 unimer at dilute conditions was available from recent small-angle neutron scattering (SANS) measurements.[49] The value of R_g = 2.19 ± 0.04 nm, obtained from the simulation, is in good agreement with the experimental value of ∼1.95 ± 0.2 nm at 293 K.[49] Pluronic F38 has a considerably bigger R_g than the one for P85 because of longer PEO blocks. L64 has the smallest value due to short PEO blocks. R_g values of PPO blocks were also calculated (Table 5). P85 shows the largest value of 1.15 nm for PPO block. This value is comparable to the thickness (1.65 nm) of the hydrophobic part of lipid bilayer. For F38 and L64, the R_g values of the PPO blocks (0.82 and 1.03 nm, respectively) are both shorter than the bilayer leaflet, especially for F38. Therefore, from these values, we expect (as the experimental results also suggest)[9] that P85 can span its PPO block through the lipid bilayer while for L64 and F38 it is less likely to happen.

DME and DMP with DMPC Bilayer. These simulations were used to test the CG force field against atomistic simulations of the same system. Therefore, we simulated DME and DMP with DMPC lipid bilayer in the same conditions as reported in our previous study.[50]

Starting with simulation of one DME/DMP inside tail groups and on top of the bilayer, we calculated the density profiles for both molecules (shown in Figure 2) at different simulation times of 5, 50, and 200 ns. For simulations starting with single DME/DMP molecule located inside the tail groups, the density profiles at 5 ns (equivalent to 50 ns of atomistic simulation) follow the same trend as the atomistic simulations.[50] The DME molecule was mostly localized in the head-group region and less in the water region, while DMP prefers to remain in the tail-group region. After 50 ns of CG simulation, the density profiles remain similar to those at 5 ns. However, after 200 ns, the DMP density profile shows the presence of the molecule also outside the bilayer in the water region. This shows that DMP molecule can diffuse in water in a time range of hundreds of microseconds. This behavior stems from the fact that DMP, as shortest oligomer of PPO, is still soluble in water.[45]

We also tested the density profiles for the DME/DMP molecules localized in the water phase on the top of the lipid bilayer. Again, the results are consistent with the atomistic simulations within 5 ns of simulations as shown in Figure 2. After 50 and 200 ns, DME and DMP densities show their better localization in the head and tail groups, respectively.

The effect of the concentration was tested by simulations of nine DME or DMP molecules on top of bilayer. Figure 3 shows

dx.doi.org/10.1021/jp306565e | J. Phys. Chem. B 2012, 116, 14333−14345

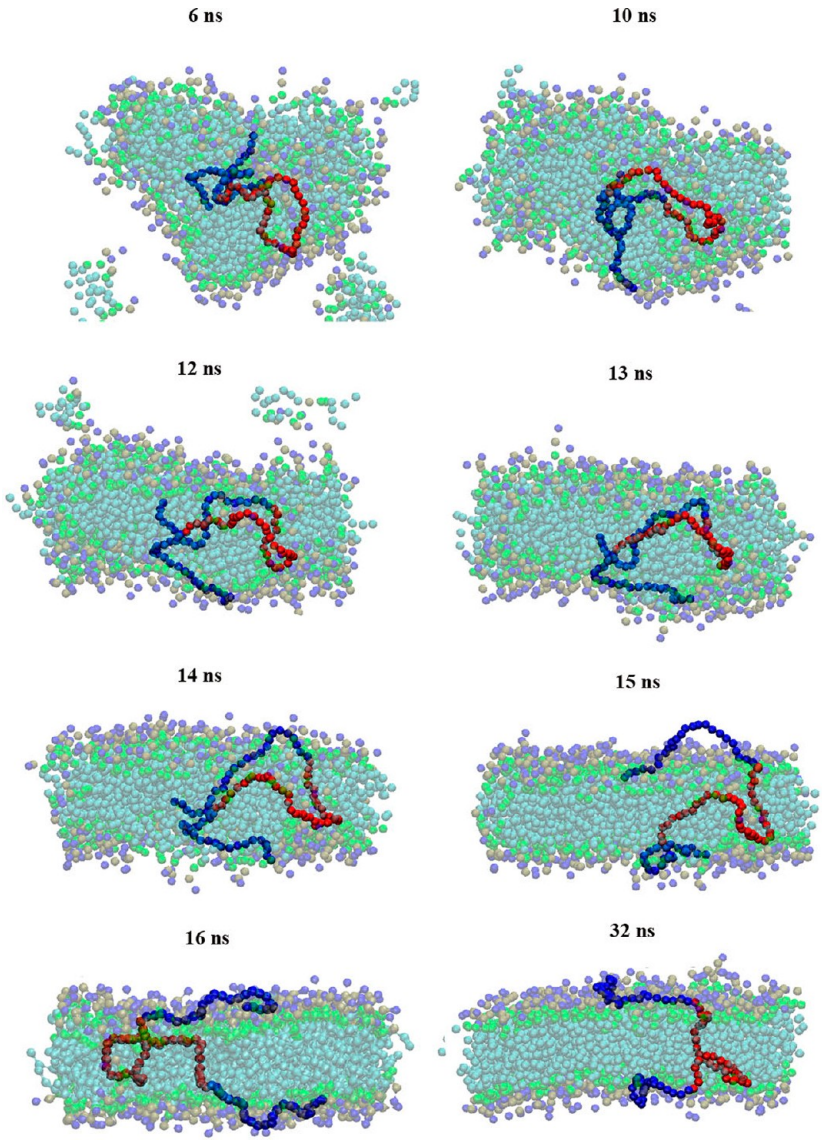

Figure 6. Snapshots of time frames along the simulation of P85 in a random mixture of water and lipid. For clarity, water molecules are not shown.

the snapshots of the simulations at 0 ns and after 400 ns. The density profiles presented in Figure 4 were calculated for 5, 50, 200, and 400 ns. Consistent with atomistic simulations, after 5 ns, a partial penetration of DMEs and DMPs into lipid bilayer head and tail groups, respectively, was observed. The density profiles become more pronounced after 50 ns in these two lipid regions. After 200 ns, a complete localization of the molecules in head groups for DME and in tail regions for DMP was observed.

Finally, for the DME and DMP oligomers, we have compared potential mean force (PMF) profiles of permeation through the lipid bilayer, using umbrella sampling from atomistic simulations,[50] with those obtained in the same manner from CG simulations. The results of this comparison show as expected a fair agreement for the DME but a larger difference for the DMP (see Figure 6S in the Supporting Information). In our CG model, DMP has a stronger relative affinity for the lipid part due to the Lennard-Jones interaction energy with the lipid tail beads. Attempts to improve the relative agreement between the atomistic and the CG for DMP by changing the interaction parameters with the lipid bilayer resulted in a reduced interaction tendency of PPO block of Pluronics chain with the tail region of the lipid bilayer (data not reported). This behavior was in contradiction with the results of our atomistic simulations and with the experimental data; therefore, we resolved to use the original parameters. It is likely that the approximate model of DMP does not account the entropic difference with the DME due to its different structure. The change of the enthalpic term alone cannot account for the correct thermodynamics of the percolation process. On the other hand, the difference observed between the atomistic and CG model PMF curve is of the order of ~15 kJ/mol, which is in the same order of magnitude observed in the comparison of atomistic PMF versus the MARTINI CG one for the extraction of single lipid from the bilayer (see Figure 5 in ref 44).

Random Ternary Mixture of Polymers, Phospholipids and Water Molecules. *Simulation of Single Pluronic Chain.* In this part of the study, we have simulated a single chain of Pluronics L64, P85, and F38 in ternary mixtures (details are reported in the Methods section). According to the experimental work of Firestone et al.,[4] the PPO and PEO length affects the interaction of polymers with DMPC lipid bilayer. From their SAXS results, they suggested two possible interactions between Pluronic and bilayer, which mainly depend on the PPO block

dx.doi.org/10.1021/jp306565e | J. Phys. Chem. B 2012, 116, 14333−14345

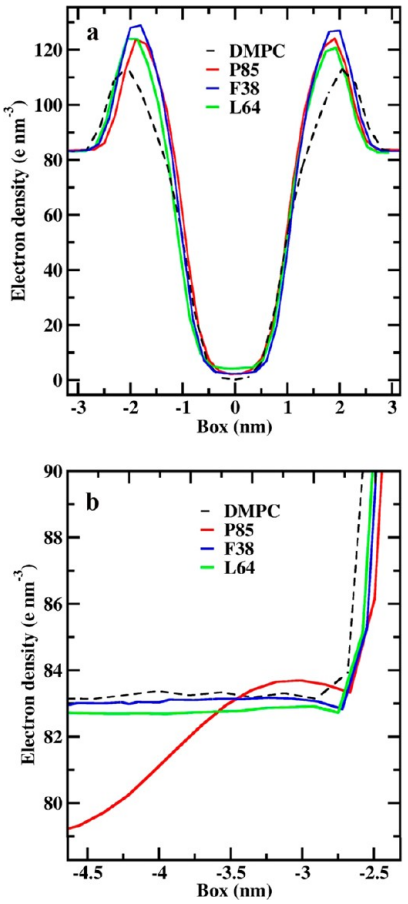

Figure 7. Electronic density profile for DMPC bilayer with Pluronics. The dashed line shows the electron density of phosphate groups and water. The total density range is from −4.5 to +4.5 that for clarity is divided into two parts, one for the membrane region (top) and one for the water region (bottom).

length. In the case of PPO block length less than the bilayer hydrophobic length, their experimental data suggested a partial insertion of PPO block in the lipid bilayer. In the other case, when the length is comparable or longer than of bilayer hydrophobic length, a complete insertion and spanning of PPO block across bilayer occurs by leaving the PEO blocks in water and on the two opposite sides of the membrane.

To verify these two scenarios with molecular models, we have considered Pluronics with different PPO block lengths such as F38, L64, and P85 and have performed simulations for 500 ns in each case. The Pluronic F38 has the shortest PPO block of 15 monomers, P85 has the longest one of 40 monomers, and L64 has the PPO block length of 30 monomers. Figure 5 shows snapshots from simulations of one polymer chain in lipid−water mixtures at 310 K right after the formation of the lipid bilayers and the equilibration of the polymer in the two-phase system.

The lipid bilayer formation is quite fast and it occurs in ∼10 to 20 ns depending on the length of the Pluronic. The simulation results suggest that PPO block is the dominant factor in interaction and insertion of Pluronic in the membrane. As we expected from R_g values of PPO blocks in water, L64 and F38 polymers show a partial insertion because of their shorter PPO blocks. On the contrary, the P85 has a PPO block long enough to cross the membrane thickness (as shown in the snapshot of Figure 5). Although the formation of the bilayer occurs quite fast, the polymer localization takes longer time after the bilayer is

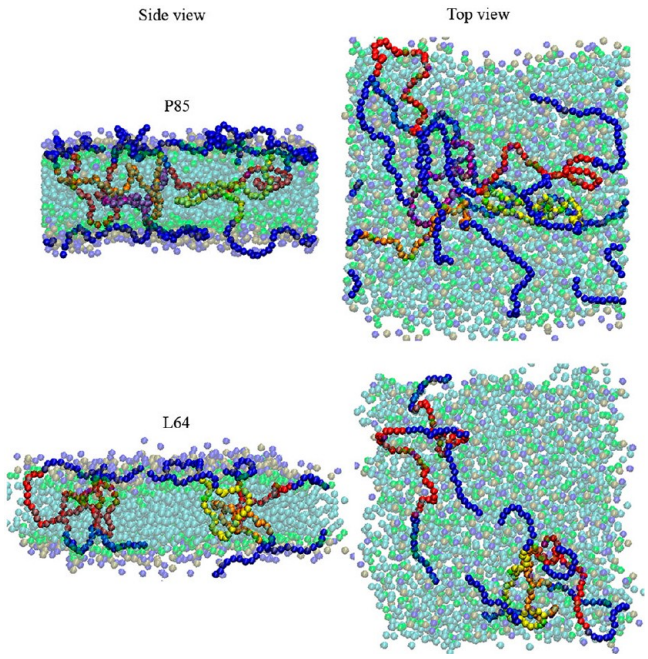

Figure 8. Snapshots from the simulations of five chains of P85 or L64 with DMPC bilayer. The snapshots are shown from top and side views. For clarity, the PPO blocks are shown in different colors and water molecules are not shown.

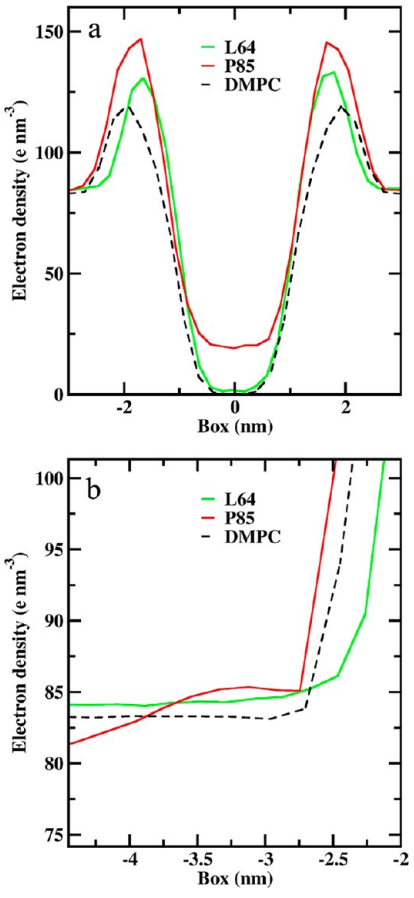

Figure 9. Electronic density profile obtained from the simulations of DMPC bilayer in the presence of five chains of Pluronics. Detail of the membrane region (top) and of the water region (bottom). The DMPC curve contains also the water density.

dx.doi.org/10.1021/jp306565e | J. Phys. Chem. B 2012, 116, 14333−14345

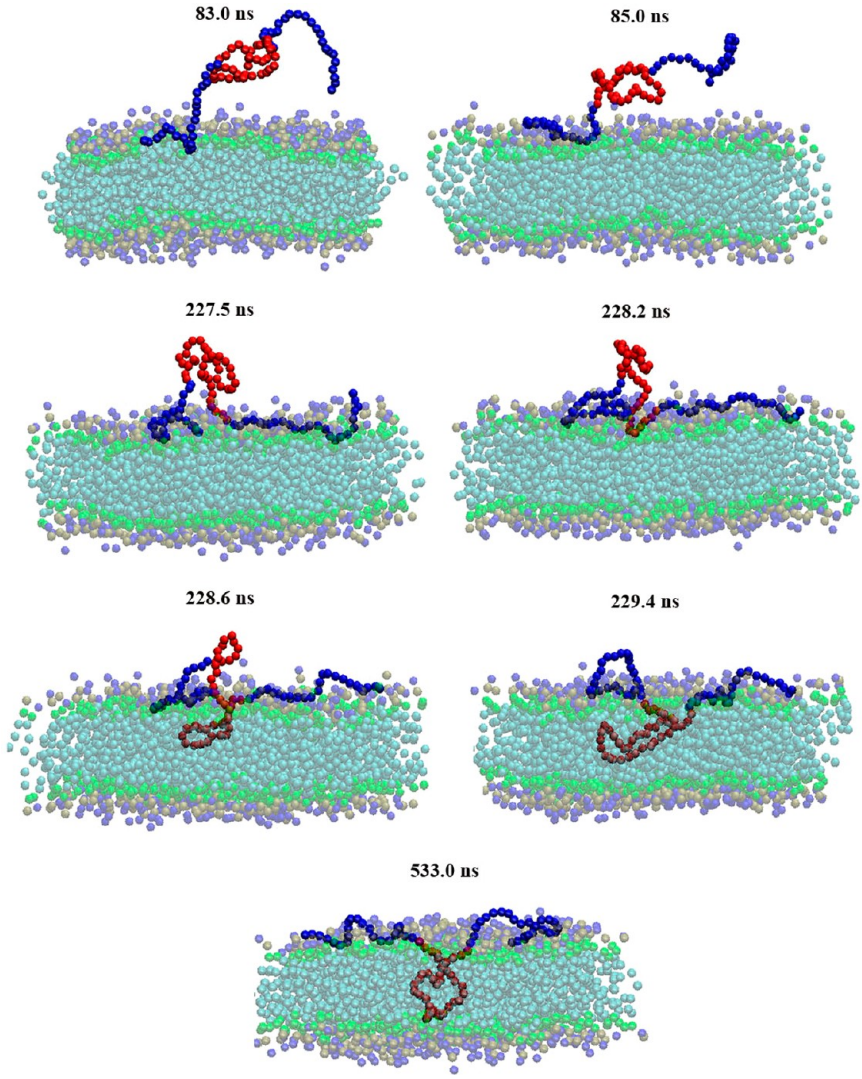

Figure 10. Different simulation time frames representing the process of interaction of P85 with DMPC bilayer and in particular the PPO block insertion into the tail region of the bilayer. Water is not shown for clarity.

formed. The polymer equilibration time depends on the PEO and PPO length. For instance, for P85, even after the lipid bilayer is formed, the two PEO blocks are still in tail groups and gradually get repelled outside in the water phase on the opposite sides of membrane. The PPO block remains completely inside as shown in last picture of Figure 6. This behavior was also reported in our previous atomistic study of DME and DMP interaction with DMPC lipid bilayer.[51]

For other Pluronics like the F38, since PPO block is shorter than the bilayer leaflet, it cannot extend completely and reach the other side of bilayer. Therefore, as both PEO blocks are repelled outside the lipid bilayer, they pull the PPO block to the same direction, and in this way, the PPO block remains inside the lipid bilayer adopting a U-shaped configuration (see Figure 5). All these results fully support the hypothesis suggested by Firestone et al.[9,33] based on their experimental results, on the possible modus of interaction of Pluronics with the DMPC lipid bilayer (see Figure 1 from the work of Firestone et al.).[9]

To evaluate these interactions more quantitatively, we have calculated the electron density for polymers and phosphate groups plus water as shown in Figure 7. The bilayer thickness, d_B, with and without the presence of Pluronics, was calculated from electron density profiles using phosphates peak-to-peak distances. The value of d_B without Pluronics was 4.01 nm, whereas in the presence of L64, P85, and F38 the distances were reduced to 3.40, 3.21, and 3.43 nm (errors are less than 0.01 nm), respectively (Figure 7 a). The decrease of the d_B values clearly indicates a bilayer thinning effect due to the presence of the polymers. The thinning effect was also observed from Lee and Firestone experimental results.[33] In addition, the electron density in water (Figure 7b) is also qualitatively comparable to the experimental results for different PEO lengths.[33] This part is mainly a region of localization of PEO into water region. In this region, P85 shows a peak at ~3.25 nm and proves more PEO localization on the surface of bilayer. This is while F38 is showing broader feature and in case of L64 there is no pronounced peak.

The area per lipid was calculated for the bilayer with and without the polymers. The value of area per lipid for pure bilayer resulted in 0.62 nm^2. However, the value increased to 0.66 nm^2 for P85 and 0.64 nm^2 for both L64 and F38 (Figure 4S in the Supporting Information). The errors in all cases are smaller than 0.01 nm^2. The slightly increase of the area per lipid is consistent with the thinning effect.

Simulations of Multiple Pluronic Chains. To test the effect of the Pluronic concentration on the lipid bilayer, 5 chains of

dx.doi.org/10.1021/jp306565e | J. Phys. Chem. B 2012, 116, 14333−14345

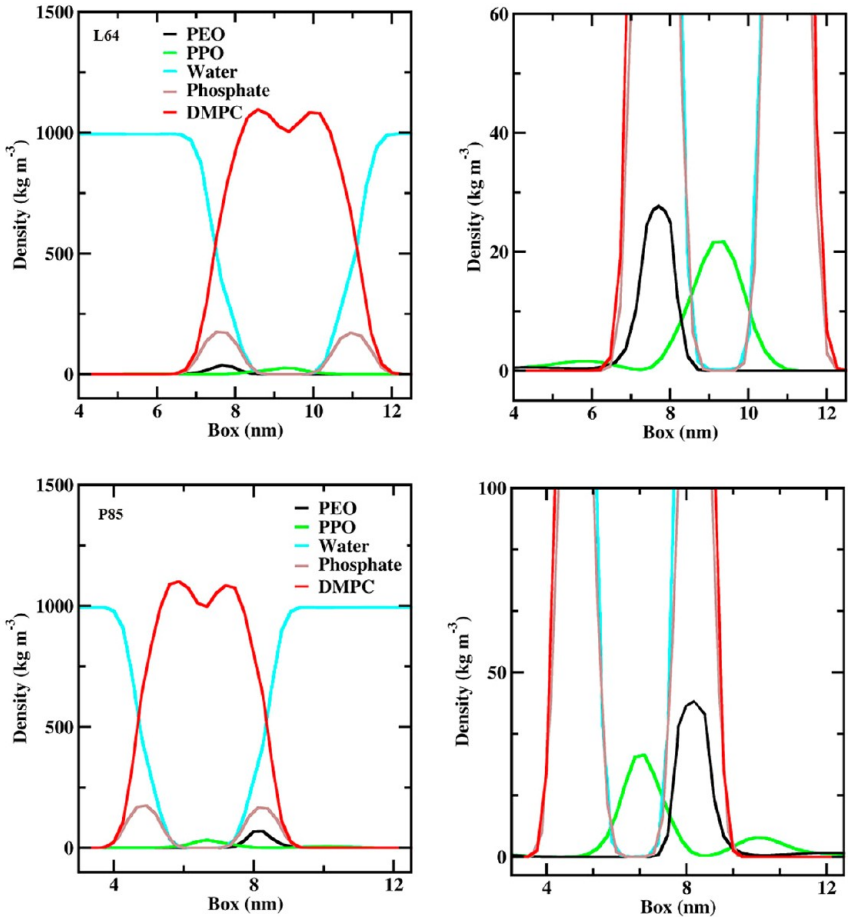

Figure 11. Density profiles from the simulation of L64 or P85 with DMPC bilayer. Density of PEO and PPO blocks in each Pluronic were calculated separately. On the right, the same plots are scaled to better evidence the PPO and PEO density.

Pluronics L64 and P85, respectively, were simulated with random lipids and on the top of the DMPC lipid bilayer.

Figure 8 shows the configuration of the systems after ~500 ns of simulation. The formation of lipid bilayer took only ~20 ns. As shown in the figure, some P85 chains did not completely extend through the bilayer. For both Pluronics, the PPO blocks of the different chains inside the bilayer tend to aggregate.

In Figure 9, the calculated electron densities for phosphate head groups, Pluronic, and water are shown. The average bilayer thicknesses were 3.10 and 3.02 nm (errors are less than 0.01) for L64 and P85, respectively. These values are 9−6% smaller than those for single-chain simulations, evidencing a concentration dependence of the bilayer thinning effect. In the water region (Figure 9b), the P85 density drops down moving away from bilayer surface, while for L64 the density shows a broader distribution. The calculated area per lipid increased up to 0.66 ± 0.01 nm^2 and 0.71 ± 0.01 nm^2 for bilayer with L64 and P85, respectively (Figure 4S in the Supporting Information). These values suggest that area per lipid increases with the length of the polymer.

Polymer on the Top of a Preformed DMPC Lipid Bilayer. *Simulation of Single Pluronic Chain.* In this part, the results of the simulations of P85 and L64 Pluronic chains with a preformed DMPC bilayer are reported. The aim of these sets of simulations was to understand the process and spontaneous diffusion of the polymer through the bilayer within the time scale of our simulations. The polymers were positioned in the water phase ~1−2 nm away from the bilayer surface and then simulated for 900 ns. Figure 10 shows snapshots from different stages of the simulation of P85 with DMPC bilayer (the results for L64 are shown in Figure 5S in the Supporting Information). The figure shows that the adsorption of the PEO block in the membrane surface is the first stage for the polymer interaction. The second stage is characterized by the percolation of the PPO block through the head groups of the lipid bilayer. The second process is quite fast and it occurs in about 2 ns. This process starts with PPO block getting in contact with the surface of bilayer (Figure 10). However, it takes 227.5 ns for PPO to get close to surface area of the bilayer. Hence, the polymer penetrates in less than 1 ns into the bilayer head-group region and comes in contact with the hydrophobic lipid tails. From this point, the insertion of the whole chain occurs in ~1 ns. Once the PPO block is completely inside the lipid bilayer (533.0 ns), it remains there for the rest of the simulation (~400 ns more), whereas PEO block remains on the bilayer surface.

In Figure 11, the density profiles for L64 (entering from the left side of the bilayer) and P85 (entering from the right side of the bilayer) before and after the insertion of PPO in the lipid bilayer are reported. The density profiles indicate that PEO mainly remains in the head-group region while PPO penetrates in the tail-group region of the bilayer. The penetration of PPO in tail groups is more extended for P85 than L64 because of longer PPO block. For both cases, PPO densities near head groups are very low. This is due to the fast insertion of the PPO block from the water phase to the bilayer inner part. As shown in the Figure 11, after PPO inserts the tails, it becomes less compact. In Table 6, the average values of R_g of Pluronics PPO blocks, inside and outside

dx.doi.org/10.1021/jp306565e | J. Phys. Chem. B 2012, 116, 14333−14345

Table 6. Radius of Gyration Values for PPO Blocks Inside and Outside Bilayer at 310 K

	R_g (nm)	
	P85	L64
outside bilayer	0.96 ± 0.04	0.93 ± 0.03
inside bilayer	1.59 ± 0.12	1.30 ± 0.03

the lipid bilayer, are reported. In Figure 12, the time series of the same R_g are also shown. Dashed lines indicate the times at which PPO block is completely inside the bilayer. The dashed lines for L64 and P85 are located at 86 and 219 ns, respectively. From Table 6 and Figure 12, it is evident that PPO R_g increases when polymers insert into the bilayer.

In these simulations, only the partial interaction of the Pluronic with lipid bilayer was observed. For P85, despite the long PPO block, a complete insertion of the block, even after the extension of the simulation up to ~2 μs, was not observed. This was due to the high hydrophobic barrier for the hydrophilic PEO, which in the simulation conditions cannot be overcome. Experimental studies have shown that other mechanisms may be involved with the interaction of the Pluronics with biological membrane that can help the translocation of PEO block from one side to the other of the lipid bilayer.[24,52] One proposed mechanism involved is an increase in the flip-flop movement of individual lipid molecules upon the interaction of Pluronics with the head groups.[24] Since these processes are supposed to occur at very slow rate (average lifetime from several hours to several days),[53,54] they could not be observed in our simulations.

Simulations of Multiple Pluronic Chains. In Figure 13, snapshots from the simulations show the interactions of five L64 and P85 Pluronic chains with a DMPC bilayer. At the beginning

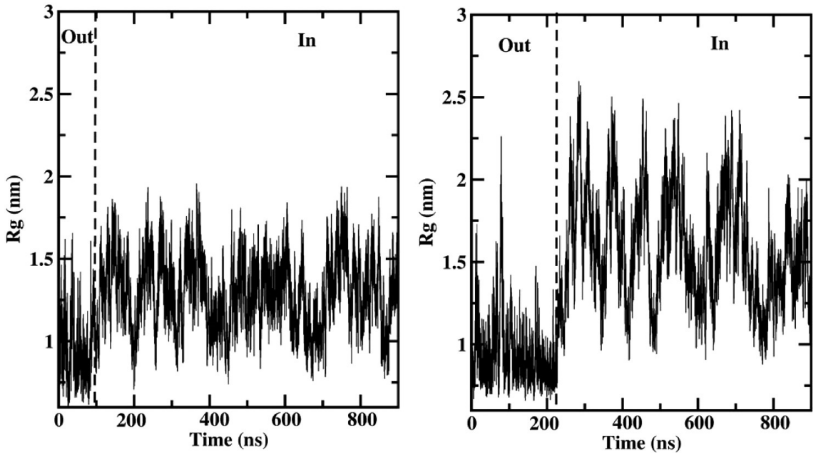

Figure 12. Time series of PPO block R_g vs time for L64 (left) and P85 (right). Dashed lines indicate the time the time at which PPO block insert completely inside the bilayer.

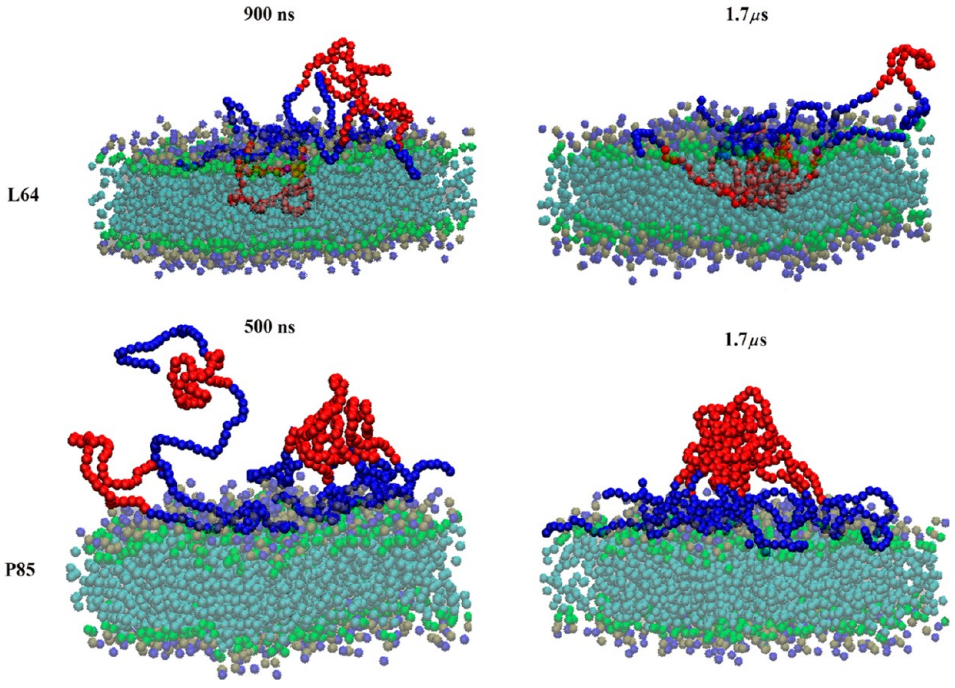

Figure 13. Different simulation time frames representing the process of interaction of five Pluronics chains located at the beginning of the simulation on the top of the DMPC bilayer. Water is not shown for clarity.

dx.doi.org/10.1021/jp306565e | J. Phys. Chem. B 2012, 116, 14333−14345

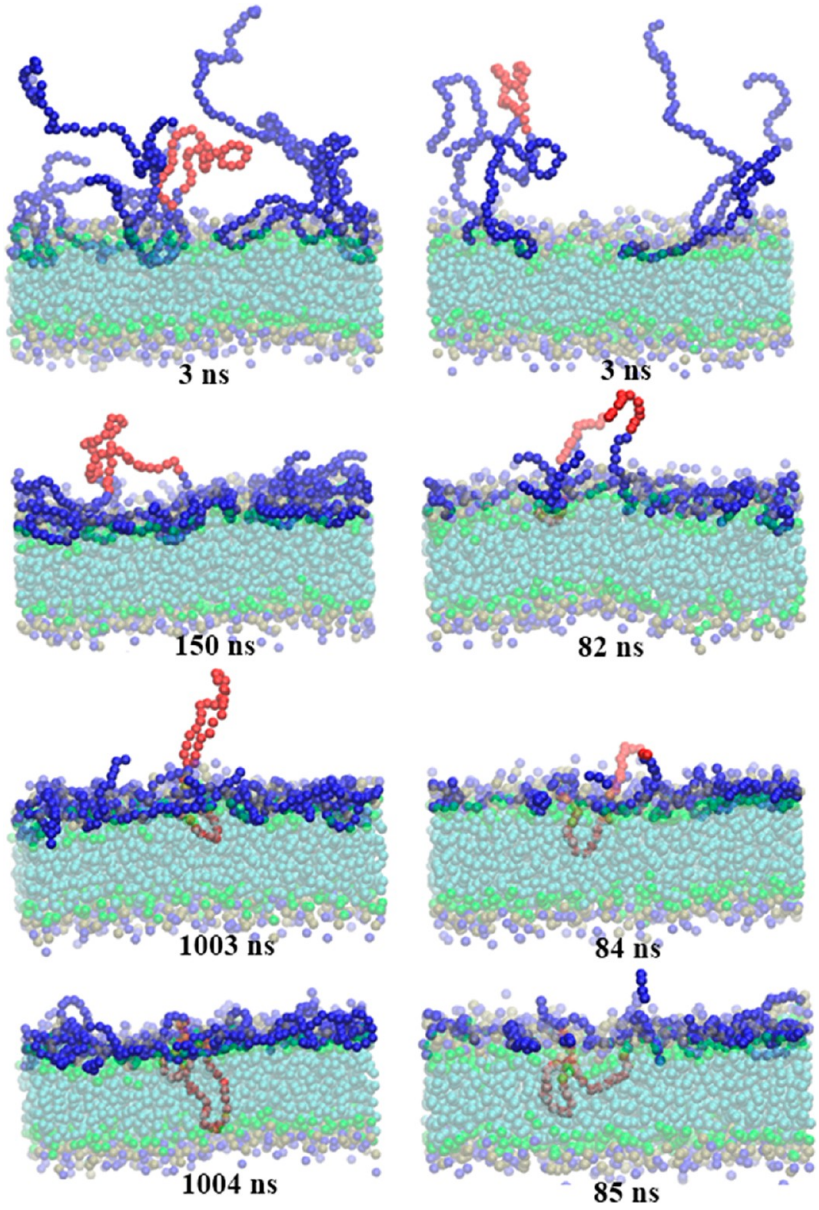

Figure 14. Different simulation time frames representing the process of interaction of one Pluronic chain plus four PEO chains located at the beginning of the simulation on the top of the DMPC bilayer. In first column snapshots from the P85 and in the second from L64 simulations are reported, respectively. Water is not shown for clarity.

of the simulations, formation of aggregates was observed for both L64 and P85 chains. The aggregation involved the formation of a PPO core that remained exposed to the water phase while the PEO parts coated the bilayer surface as shown in the Figure 13. This process delayed the insertion of individual chains into the lipid bilayer and, after 900 ns, only two L64 chains were able to insert their PPO blocks inside the membrane and the other two L64 chains inserted only after 1.7 μs. For P85 chains, even after 1.7 μs no insertion was observed (Figure 13, at 1.7 μs).

Comparing the two simulations, it seems that the length of PEO is an important factor in the way Pluronics interact with the lipid bilayer, especially when the polymer concentration increases. In particular, the PPO entanglement also seems to play a role in percolation rate. To check whether this delay is due to the PEO surface coating or the PPO entanglement, further simulations were performed with four PEO chains (with the same length of Pluronics L64 and P85) and only one Pluronic chain. In Figure 14, the system A includes PEO chains and P85 while system B contains PEO chains and L64. System A contains around 1.6 times more PEO chains than B. In this way, we could figure out the role of PEO surface coating without the effect of PPO entanglement. The results of the simulation showed that the PPO block of Pluronic L64 could penetrate into the lipid bilayer in ~85 ns, which is very close to the first passage time observed from the simulation of the single L64 chain (see Figure 5S in the Supporting Information). However, for the P85 the insertion occurred around 1 μs, which is ~4 times longer than the time required for the isolated chain (229.4 ns, see also Figure 10). From these simulations, it seems clear that both PPO entanglement and PEO surface coating play a role in the rate of permeation of the polymer into the lipid bilayer. In fact, the relative higher concentration of the PEO blocks and the PPO aggregation can both prevent the contact of PPO blocks with the bilayer surface and, therefore, reduce the insertion rate. This interesting

dx.doi.org/10.1021/jp306565e | J. Phys. Chem. B 2012, 116, 14333−14345

finding about effect of PEO coating supports the experimental fluorescent microscopy measurements[31] that show the absence of diffusion through cellular membrane for Pluronics with long PEO blocks. Our simulations have also showed, however, the PPO entanglements may play a role in this process.

CONCLUSIONS

This work was aimed to understand the interaction of poloxamers at the molecular level with lipid bilayer using coarse-grained simulations based on the MARTINI force field. The CG model for Pluronics was parametrized using simulation data of previously reported atomistic model.[42,45] The CG models of PEO, PPO, and Pluronics show good agreement with the atomistic simulation data as well as with the experimentally determined properties of these polymers in water (i.e., radius of gyration).

We have modeled and studied the interaction of Pluronics with DMPC lipid bilayer. The results of the study are consistent with experimental SAXS data and provide molecular details of the interaction. First, the role of PPO block length was shown as a critical determinant of the mode of insertion of the copolymer in the lipid bilayer. A poor permeation of the polymer was observed for PPO block lengths less than the bilayer leaflet while allowing the PEO chains to extend on the top of the lipid bilayer. On the contrary, when the PPO block has a length comparable to the bilayer thickness, it can span across the lipid bilayer with the PEO blocks flanking on the opposite sides of bilayer in the water phase. Second, the calculated electron density profiles evidence a thinning effect of Pluronics on the bilayer, which is consistent with the experimental SAXS data. This effect is followed by an increase in the area per lipid. Our results indicate that DMPC lipid bilayer in the presence of Pluronics L64 or P85 tends to be more permeable with a more evident effect for the P85.

Simulations of Pluronics on top of the lipid bilayer were used to reproduce the actual phenomenon of interaction of polymer with biological membranes. The results of these simulations indicate that the process mainly proceeds by a two-stage mechanism. First, the PEO gets adsorbed on the hydrophilic surface of the membrane. This makes the PPO block to get close to the bilayer surface. Second, while the PEO remains close to the head groups of the lipid bilayer, the PPO starts penetrating inside the tail regions. Interestingly, as the polymer concentration increases, the rate of diffusion of the polymer in the bilayer tail region slows down. Our simulations indicate that this effect can be caused due to both the PEO concentration and the PPO block aggregation that delays and, in case of longer chains, prevents the contact of PPO blocks with the bilayer surface, thus reducing the chance of their insertion. This finding is consistent with the experimental studies[31] showing the interactions of Pluronics with long PEO blocks are only limited to the covering of the membrane surfaces.

ASSOCIATED CONTENT

Supporting Information

The details of MARTINI CG force field parametrization and validation and figure for interaction of Pluronic L64 with DMPC bilayer. This material is available free of charge via the Internet at http://pubs.acs.org.

AUTHOR INFORMATION

Corresponding Author

*Fax: +39 0899 65296 (G.M.); +49 421 2003249 (D.R.). Tel.: +39 089 969567 (G.M.); +49 421 2003144 (D.R.). E-mail: gmilano@unisa.it (G.M.); d.roccatano@jacobs-university.de (D.R.).

Notes

The authors declare no competing financial interest.

ACKNOWLEDGMENTS

This project is funded by the Deutsche Forschungsgemeinschaft (DFG) for the project titled "The Study of Detailed Mechanism of Polymers/Biological Membrane Interactions Using Computer Simulation" (RO 3571/3-1).

REFERENCES

(1) Xin, X.; Xu, G. Y.; Zhang, Z. Q.; Chen, Y. J.; Wang, F. *Eur. Polym. J.* **2007**, *43*, 3106.
(2) Chiappetta, D. A.; Sosnik, A. *Eur. J. Pharm. Biopharm.* **2007**, *66*, 303.
(3) Escobar-Chavez, J. J.; Lopez-Cervantes, M.; Naik, A.; Kalia, Y. N.; Quintanar-Guerrero, D.; Ganem-Quintanar, A. *J. Pharm. Pharm. Sci.* **2006**, *9*, 339.
(4) Kabanov, A. V.; Batrakova, E. V.; Alakhov, V. Y. *Adv. Drug Delivery Rev.* **2002**, *54*, 759.
(5) Wasungu, L.; Marty, A. L.; Bureau, M. F.; Kichler, A.; Bessodes, M.; Teissie, J.; Scherman, D.; Rols, M. P.; Mignet, N. *J. Controlled Release* **2011**, *149*, 117.
(6) Fusco, S.; Borzacchiello, A.; Netti, P. A. *J. Bioact. Compat. Polym.* **2006**, *21*, 149.
(7) Erukova, V. Y.; Krylova, O. O.; Antonenko, Y. N.; Melik-Nubarov, N. S. *Biochim. Biophys. Acta, Biomembr.* **2000**, *1468*, 73.
(8) Frey, S. L.; Zhang, D. S.; Carignano, M. A.; Szleifer, I.; Lee, K. Y. C. *J. Chem. Phys.* **2007**, *127*.
(9) Firestone, M. A.; Wolf, A. C.; Seifert, S. *Biomacromolecules* **2003**, *4*, 1539.
(10) Maskarinec, S. A.; Wu, G. H.; Lee, K. Y. C. *Cell Inj.: Mech., Responses, Repair* **2005**, *1066*, 310.
(11) Amado, E.; Blume, A.; Kressler, J. *React. Funct. Polym.* **2009**, *69*, 450.
(12) Amado, E.; Kressler, J. *Curr. Opin. Colloid Interface Sci.* **2011**, *16*, 491.
(13) Peetla, C.; Stine, A.; Labhasetwar, V. *Mol. Pharm.* **2009**, *6*, 1264.
(14) Carlsson, M.; Hallen, D.; Linse, P. *J. Chem. Soc., Faraday Trans.* **1995**, *91*, 2081.
(15) Amado, E.; Kerth, A.; Blume, A.; Kressler, J. *Langmuir* **2008**, *24*, 10041.
(16) Hussain, H.; Kerth, A.; Blume, A.; Kressler, J. *J. Phys. Chem. B* **2004**, *108*, 9962.
(17) Frey, S. L.; Lee, K. Y. C. *Langmuir* **2007**, *23*, 2631.
(18) Feitosa, E.; Winnik, F. M. *Langmuir* **2010**, *26*, 17852.
(19) Chieng, Y. Y.; Chen, S. B. *J. Phys. Chem. B* **2009**, *113*, 14934.
(20) Wu, G. H.; Khant, H. A.; Chiu, W.; Lee, K. Y. C. *Soft Matter* **2009**, *5*, 1496.
(21) Schulz, M.; Olubummo, A.; Binder, W. H. *Soft Matter* **2012**, *8*, 4849.
(22) Binder, W. H. *Angew. Chem., Int. Ed.* **2008**, *47*, 3092.
(23) Kabanov, A. V.; Batrakova, E. V.; Miller, D. W. *Adv. Drug Delivery Rev.* **2003**, *55*, 151.
(24) Krylova, O. O.; Pohl, P. *Biochemistry* **2004**, *43*, 3696.
(25) Miller, D. W.; Batrakova, E. V.; Kabanov, A. V. *Pharm. Res.* **1999**, *16*, 396.
(26) Wu, G. H.; Majewski, J.; Ege, C.; Kjaer, K.; Weygand, M. J.; Lee, K. Y. C. *Biophys. J.* **2005**, *89*, 3159.
(27) Majewski, J.; Kuhl, T. L.; Wong, J. Y.; Smith, G. S. *Rev. Mol. Biotechnol.* **2000**, *74*, 207.
(28) Castile, J. D.; Taylor, K. M. G.; Buckton, G. *Int. J. Pharm.* **2001**, *221*, 197.
(29) Heerklotz, H.; Seelig, J. *Biochim. Biophys. Acta, Biomembr.* **2000**, *1508*, 69.
(30) Pembouong, G.; Morellet, N.; Kral, T.; Hof, M.; Scherman, D.; Bureau, M. F.; Mignet, N. *J. Controlled Release* **2011**, *151*, 57.
(31) Maskarinec, S. A.; Hannig, J.; Lee, R. C.; Lee, K. Y. C. *Biophys. J.* **2002**, *82*, 1453.

(32) Firestone, M. A.; Seifert, S. *Biomacromolecules* **2005**, *6*, 2678.
(33) Lee, B.; Firestone, M. A. *Biomacromolecules* **2008**, *9*, 1541.
(34) Wang, J. Y.; Chin, J. M.; Marks, J. D.; Lee, K. Y. C. *Langmuir* **2010**, *26*, 12953.
(35) Wang, Q. F.; Keffer, D. J.; Nicholson, D. M. *J. Chem. Phys.* **2011**, *135*.
(36) Lee, H.; de Vries, A. H.; Marrink, S. J.; Pastor, R. W. *J. Phys. Chem. B* **2009**, *113*, 13186.
(37) Bedrov, D.; Ayyagari, C.; Smith, G. D. *J. Chem. Theory Comput.* **2006**, *2*, 598.
(38) Fischer, J.; Paschek, D.; Geiger, A.; Sadowski, G. *J. Phys. Chem. B* **2008**, *112*, 13561.
(39) Hatakeyama, M.; Faller, R. *Phys. Chem. Chem. Phys.* **2007**, *9*, 4662.
(40) Nawaz, S.; Redhead, M.; Mantovani, G.; Alexander, C.; Bosquillon, C.; Carbone, P. *Soft Matter* **2012**, *8*, 2744.
(41) Kawaguchi, S.; Imai, G.; Suzuki, J.; Miyahara, A.; Kitano, T. *Polymer* **1997**, *38*, 2885.
(42) Stubbs, J. M.; Potoff, J. J.; Siepmann, J. I. *J. Phys. Chem. B* **2004**, *108*, 17596.
(43) Marrink, S. J.; de Vries, A. H.; Mark, A. E. *J. Phys. Chem. B* **2004**, *108*, 750.
(44) Marrink, S. J.; Risselada, H. J.; Yefimov, S.; Tieleman, D. P.; de Vries, A. H. *J. Phys. Chem. B* **2007**, *111*, 7812.
(45) Hezaveh, S.; Samanta, S.; Milano, G.; Roccatano, D. *J. Chem. Phys.* **2011**, *135*.
(46) Hess, B.; Kutzner, C.; van der Spoel, D.; Lindahl, E. *J. Chem. Theory Comput.* **2008**, *4*, 435.
(47) Berendsen, H. J. C.; Postma, J. P. M.; Vangunsteren, W. F.; Dinola, A.; Haak, J. R. *J. Chem. Phys.* **1984**, *81*, 3684.
(48) Flyvbjerg, H.; Petersen, H. G. *J. Chem. Phys.* **1989**, *91*, 461.
(49) Hammouda, B. *Eur. Polym. J.* **2010**, *46*, 2275.
(50) Samanta, S.; Hezaveh, S.; Milano, G.; Roccatano, D. *J. Phys. Chem. B* **2012**, *116*, 5141.
(51) Hager, S. L.; Macrury, T. B. *J. Appl. Polym. Sci.* **1980**, *25*, 1559.
(52) Yaroslavov, A. A.; Melik-Nubarov, N. S.; Menger, F. M. *Acc. Chem. Res.* **2006**, *39*, 702.
(53) Kornberg, R. D.; Mcconnel, Hm. *Biochemistry* **1971**, *10*, 1111.
(54) Wimley, W. C.; Thompson, T. E. *Biochemistry* **1990**, *29*, 1296.